

# INTERPRETATION OF SUBCRITICAL SOURCE-DRIVEN NOISE ANALYSIS MEASUREMENTS

Timothy E. Valentine  
Oak Ridge National Laboratory  
P. O. Box 2008, Oak Ridge, TN 37831-6354  
Fax: 1-865-574-6182, e-mail: valentinete@ornl.gov

## ABSTRACT

The interpretation of subcritical source-driven noise analysis measurements had previously relied upon the use of point reactor kinetic models to relate the measured quantities to the neutron multiplication factor  $k_{eff}$ . Monte Carlo codes have been developed that can directly simulate the source-driven noise analysis measurement in the same manner in which the measurement is performed. The Monte Carlo codes can be used to interpret the measurements to determine the subcritical neutron multiplication factor using a perturbation technique that has been analytically developed. This paper demonstrates how source-driven subcritical noise analysis measurements with a highly enriched uranyl nitrate solution system are interpreted using the Monte Carlo technique. The measurements were interpreted using a variety of perturbations with several nuclear cross section data sets to demonstrate that the interpretation methodology is not significantly dependent on the perturbation and does not depend significantly on the nuclear cross section data. The largest difference among the interpreted  $k_{eff}$  values is 0.003 for the nuclear cross section data sets used in this analysis.

## 1. INTRODUCTION

Subcritical measurements were developed to study the dynamic behavior of neutrons in a fissile system. One common aspect of this was to determine the neutron multiplication factor. Interpretation of measurements requires some model to relate what is measured to  $k_{eff}$ . In the past, the subcritical noise measurements were interpreted using equations developed from point kinetics models for the time-dependent behavior of neutrons in the subcritical configuration. This limited the application of the measurement to situations in which point kinetics was applicable. The source-driven noise analysis measurement[1] was developed to overcome some of the limitations of other subcritical measurement techniques, but interpretation of the measurements was dependent on the applicability of the point reactor kinetics models. The most general model to relate the measured quantities to  $k_{eff}$  would involve the use of the generalized stochastic model developed by Munoz-Cobos et al.[2]

Although an analytical solution of subcritical noise measurements in terms of the stochastic model is not practical, the Monte Carlo method provides a means to simulate the subcritical measurements and to also calculate  $k_{eff}$ . In fact, the same Monte Carlo code and nuclear data can be used for simulation of subcritical measurements and for  $k_{eff}$  calculation. The Monte Carlo code MCNP-DSP[3] was developed to simulate a variety of subcritical measurement methods and can be used to simulate directly the source-driven noise analysis measurement.

Furthermore, Perez et al[4] demonstrated that a first order perturbation technique could be used to interpret the source-driven noise analysis measurement using the Monte Carlo method.

A brief review of the measurement method and the simulation of the measurements is provided in Section 2. A brief review of the interpretation methodology as developed by Perez et al is provided in Section 3. A description of the simulation of measurements with a uranyl nitrate solution system and the results of the analysis are presented in Section 4. Finally, concluding remarks are provided in Section 5.

## 2. SOURCE-DRIVEN NOISE ANALYSIS MEASUREMENTS AND SIMULATIONS

Subcritical source-driven noise measurements are simultaneous Rossi- $\alpha$  and randomly pulsed neutron measurements that provide measured quantities that can be related to  $k_{eff}$ . The source-driven noise analysis measurement requires the use of a timed neutron source such as a  $^{252}\text{Cf}$  source ionization chamber (detector 1) and two or more neutron detectors (detectors 2 and 3, respectively). The time-dependent responses,  $f(t)$ , of the source and detectors are correlated in the frequency domain to obtain auto and cross spectra. The source-detector cross spectra are designated as  $G_{12}(\omega)$  and  $G_{13}(\omega)$  and are the frequency domain equivalent of the randomly pulsed neutron measurement. The detector-detector cross spectrum is designated as  $G_{23}(\omega)$  and is the frequency domain equivalent of the two-detector Rossi- $\alpha$  measurement. The auto spectra of the source is designated as  $G_{11}(\omega)$  and is related to the spontaneous fission rate of the source. The detector auto spectra are designated as  $G_{22}(\omega)$  and  $G_{33}(\omega)$  and are the frequency domain equivalent to the single-detector Rossi- $\alpha$  measurement. A complete review of the auto and cross spectra can be found in ref. 5. A certain ratio ( $R$ ) of the frequency spectra is independent of detection efficiency and can be directly computed using Monte Carlo codes. The spectral ratio is defined as:

$$R(\omega) = \frac{G_{12}^*(\omega)G_{13}(\omega)}{G_{11}(\omega)G_{23}(\omega)}. \quad (1)$$

The asterisk in Eq. 1 denotes complex conjugation. If point reactor kinetics models are used to describe the various frequency spectra for the source-driven noise analysis measurement, the spectral ratio is related to reactivity as follows:

$$R(\omega) = \frac{\varepsilon_s \overline{\nu_0}}{\left[ \frac{\nu(\nu-1)}{\nu|\rho|} + \frac{\nu_0(\nu_0-1)}{\nu_0} \right]}. \quad (2)$$

In this expression,  $\varepsilon_s$  is the efficiency for detecting the spontaneous fission of the source,  $\nu$  is the number of neutrons from fission in the system,  $\nu_0$  is the number of neutrons from the  $^{252}\text{Cf}$  source, and  $\rho$  is the system reactivity. As can be seen from the simplified expression in Eq. 2, the spectral ratio will approach a constant value, i.e. the inverse of the Diven factor for

<sup>252</sup>Cf, as  $k_{eff}$  approaches zero. Therefore, as the  $k_{eff}$  value decreases the spectral ratio becomes less sensitive. On the other hand, as the  $k_{eff}$  value increases the spectral ratio becomes more sensitive because it is inversely related to reactivity that changes a greater rate than  $k_{eff}$ .

The Monte Carlo code MCNP-DSP was developed to simulate a variety of subcritical measurements. In MCNP-DSP, the variance reduction features were disabled to obtain a strictly analog particle tracking to follow the fluctuating processes more accurately. Because biasing techniques are typically employed to reduce the variance of estimates of first moment quantities, they do not preserve the higher moments; therefore, analog Monte Carlo calculations must be performed when analyzing subcritical measurements whose measured quantities are directly related to the higher moments of the neutron production. Because the use of average quantities reduces the statistical fluctuations of the neutron population, average quantities such as the average number of neutrons from fission are not used; instead, appropriate probability distribution functions are sampled. The prompt particle tracking begins with the source event and the subsequent fission chains are followed to extinction. Time series of pulses are obtained at the detectors for each fission chain. These sequences are sampled into blocks of 512 or 1024 data points. The blocks of data are then processed according to the type of measurement being simulated. The auto and cross spectra are computed directly from the Fourier transform of the source and detector time series for each data block. The auto and cross spectra are then averaged over many blocks to obtain the final estimates of the auto and cross spectra. The spectral ratio can then be computed from the auto and cross spectra as is done in the source-driven noise analysis measurement.

### 3. PERTURBATION TECHNIQUE FOR INTERPRETING SOURCE-DRIVEN NOISE ANALYSIS MEASUREMENTS

The Monte Carlo codes are used to interpret the measurement by performing a calculation of the measured parameters and a separate eigenvalue calculation. For example, a comparison of measured and calculated values of the spectral ratio can be used to obtain the “experimental”  $k_{eff}$ . If the measured and calculated values of the spectral ratio are in agreement, then the bias in the spectral ratio is zero. The bias in the spectral ratio is defined as the difference between measured and calculated values of the spectral ratio ( $R_m - R_c$ ) where  $R_m$  is the measured value and  $R_c$  is the calculated value. First order perturbation theory can be used to obtain an expression that can be used to determine the “experimental”  $k_{eff}$  and the bias in the  $k_{eff}$ . The low-frequency value of the spectral ratio has been shown in numerous experiments to be linear with  $k_{eff}$  over a wide range of values of  $k_{eff}$  with the values of  $k_{eff}$  being interpreted using point kinetics models. Given the linear dependence of the spectral ratio with  $k_{eff}$ , the bias in the spectral ratio varies linearly as the bias in  $k_{eff}$  ( $k_m - k_c$ ). To determine the “experimental”  $k_{eff}$  value and its bias, the Monte Carlo models are slightly perturbed and new values of the spectral ratio ( $R_p$ ) and  $k_{eff}$  ( $k_p$ ) are obtained. If the linear dependence is valid, then the perturbation calculations can be used to obtain the “experimental”  $k_{eff}$  and its bias using the following linear relationship

$$\frac{R_m - R_c}{k_m - k_c} = \frac{R_p - R_c}{k_p - k_c}. \quad (3)$$

This methodology simply uses a linear interpolation or extrapolation between the standard and perturbed values of the spectral ratio and  $k_{eff}$  to determine the “experimental”  $k_{eff}$ . Using this relationship, the value of  $k_m$  can be determined along with its bias  $k_m - k_c$ . Propagation of error is used to obtain the uncertainty in  $k_m$  and its bias. Even if the measured spectral ratio value and the calculated value agree, the perturbation analysis is performed. This is required to equate the uncertainty in the measured spectral ratio to the uncertainty in the inferred  $k_{eff}$  value.

Perez et al have demonstrated that the relationship given in Eq 3 was valid using first order perturbations of the Greens functions expressions for  $k_{eff}$  and the spectral ratio. In the paper, Perez summarized the relationships for  $k_{eff}$  and the spectral ratio in terms of a Greens function of the transport equation. By performing perturbations of the Greens function, relationships between the standard calculated values of the spectral ratio or  $k_{eff}$  could be related to the perturbed values. Perturbing the Greens function yields the following relationship between the standard and perturbed spectral ratio values

$$\frac{R_p - R_c}{R_c} = A_s (\alpha_p - 1). \quad (4)$$

In this expression  $A_s$  contains the dependency on the Greens function and  $\alpha_p$  is the ratio of the perturbed parameter to the unperturbed parameter. A similar relationship is obtained for the perturbed and standard  $k_{eff}$  values

$$\frac{k_p - k_c}{k_c} = Z_s (\alpha_p - 1). \quad (5)$$

In this expression  $Z_s$  contains the dependency on the Greens function. Note that the terms  $A_s$  and  $Z_s$  are different but both depend on the Greens function of the transport equation. The bias in the spectral ratio calculation was defined as  $R_m - R_c$  and can be equated to the uncertainty of the Greens function parameters

$$\frac{R_m - R_c}{R_c} = A_s (\alpha_m - 1). \quad (6)$$

This essentially implies that the calculated spectral ratio differs from the measured spectral ratio because the nuclear data and the Monte Carlo model do not sufficiently represent the measurement conditions. Likewise, the difference between the measured  $k_m$  and the calculated  $k_c$  could be equated to the same uncertainty of the Greens function parameters

$$\frac{k_m - k_c}{k_c} = Z_s (\alpha_m - 1). \quad (7)$$

The ratio of Eq. 6 to Eq. 4 and the ratio of Eq. 7 to Eq. 5 are equal

$$\frac{\frac{R_m - R_c}{R_c}}{\frac{R_p - R_c}{R_c}} = \frac{(\alpha_m - 1)}{(\alpha_p - 1)} = \frac{\frac{k_m - k_c}{k_c}}{\frac{k_p - k_c}{k_c}}. \quad (8)$$

The results of the perturbation analyses directly yielded Eq 3.

#### 4. ANALYSIS OF URANYL NITRATE SOLUTION MEASUREMENTS

In 1984, subcritical measurements were performed with an unreflected cylindrical tank containing uranyl nitrate using the  $^{252}\text{Cf}$ -source-driven noise analysis method[6]. The measurements consisted of filling a right circular acrylic cylinder with varying amounts of a highly enriched uranyl nitrate solution. A  $^{252}\text{Cf}$  source in a parallel plate ionization chamber was located at various axial positions along the central axis of the acrylic cylinder. Detectors were placed external to the cylindrical tank to measure neutrons and gamma rays emitted from the system. A sketch of the geometry for this system is provided in Figure 1. Measurements were performed with the source at the axial center of the solution for various solution heights and with varying source positions for fixed solution heights. The benchmark spectral ratio values[7] from these measurements are provided in Table 1.

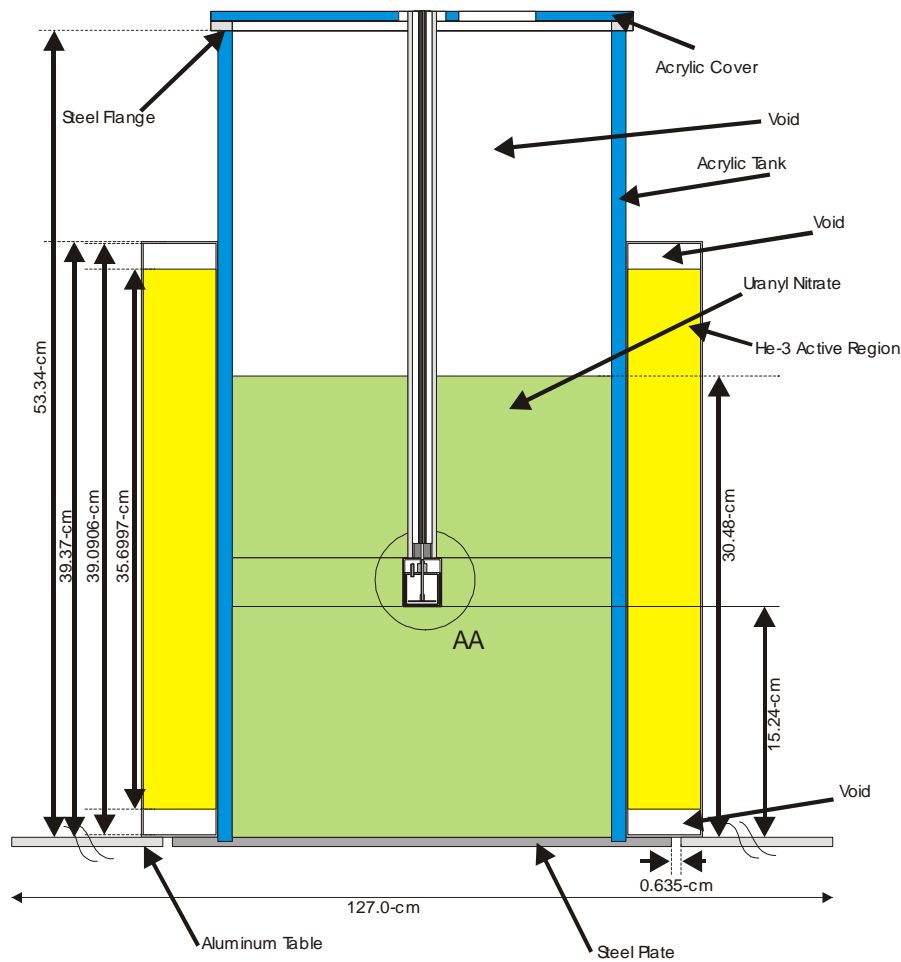


Figure 1. Sketch of uranyl nitrate solution tank with central source.

Table 1. Benchmark and Standard Model Spectral Ratio Values and Standard Model  $k_{eff}$  Values for Interpretation of Noise Analysis Measurements

Case	Solution Height (cm)	Benchmark Spectral Ratio ( $R_m$ ) ( $10^{-3}$ )	ENDF/B-V Spectral Ratio ( $R_c$ ) ( $10^{-3}$ )	ENDF/B-V Calculated ( $k_c$ ) $k_{eff}$
1	30.48	98.0 ± 12.0	105.5 ± 0.1	0.9599 ± 0.0003
2	27.94	139.0 ± 9.7	151.3 ± 0.1	0.9391 ± 0.0003
3	25.40	187.7 ± 10.6	202.9 ± 0.1	0.9141 ± 0.0003
4	22.86	248.0 ± 9.7	259.5 ± 0.3	0.8829 ± 0.0003
5	20.32	303.5 ± 9.7	328.4 ± 0.3	0.8445 ± 0.0003

Perturbations were made to the uranium density, the solution density, the tank dimensions, and the uranium enrichment. The results of a 2.0% increase in the solution density are provided in Tables 2 for the ENDF/B-V cross-section data.

Table 2. Perturbed Spectral Ratio and  $k_{eff}$  Values and Experimental  $k_{eff}$  Obtained from Perturbing the Solution Density +2.0% using ENDF/B-V Cross Sections

Case	Solution Height (cm)	Perturbed Spectral Ratio ( $R_p$ ) ( $10^{-3}$ )	Perturbed ( $k_p$ ) $k_{eff}$	“Experimental” $k_{eff}$
1	30.48	66.1 ± 0.1	0.9763 ± 0.0003	0.9630 ± 0.0050
2	27.94	113.4 ± 0.2	0.9556 ± 0.0003	0.9445 ± 0.0042
3	25.40	170.0 ± 0.2	0.9304 ± 0.0003	0.9230 ± 0.0053
4	22.86	229.7 ± 0.2	0.9000 ± 0.0003	0.8895 ± 0.0056
5	20.32	297.7 ± 0.6	0.8619 ± 0.0003	0.8586 ± 0.0055

A second perturbation was performed in which the uranium density was reduced 3% while keeping the solution density fixed. The results of this analysis are provided in Table 3. This change in the uranium density produced results similar to those obtained by increasing the solution density.

Table 3. Perturbed Spectral Ratio and  $k_{eff}$  Values and Experimental  $k_{eff}$  Obtained from Perturbing the Uranium Density -3% using ENDF/B-V Cross Sections

Case	Solution Height (cm)	Perturbed Spectral Ratio ( $R_p$ ) ( $10^{-3}$ )	Perturbed ( $k_p$ ) $k_{eff}$	“Experimental” $k_{eff}$
1	30.48	58.5 ± 0.1	0.9793 ± 0.0003	0.9630 ± 0.0049
2	27.94	108.2 ± 0.2	0.9583 ± 0.0003	0.9446 ± 0.0043
3	25.40	162.6 ± 0.1	0.9326 ± 0.0003	0.9223 ± 0.0049
4	22.86	225.0 ± 0.4	0.9028 ± 0.0003	0.8895 ± 0.0056
5	20.32	292.3 ± 0.5	0.8638 ± 0.0003	0.8578 ± 0.0052

A third perturbation was performed in which the uranium density was increased 3% while keeping the solution density fixed, and the results of the perturbation analysis are provided in Table 4.

Table 4. Perturbed Spectral Ratio and  $k_{eff}$  Values and Experimental keff Obtained from Perturbing the Uranium Density +3% using ENDF/B-V Cross Sections

Case	Solution Height (cm)	Perturbed Spectral Ratio ( $R_p$ ) ( $10^{-3}$ )	Perturbed ( $k_p$ ) $k_{eff}$	“Experimental” $k_{eff}$
1	30.48	152.3 ± 0.1	0.9396 ± 0.0003	0.9632 ± 0.0052
2	27.94	195.0 ± 0.2	0.9198 ± 0.0003	0.9445 ± 0.0043
3	25.40	245.1 ± 0.2	0.8936 ± 0.0003	0.9228 ± 0.0052
4	22.86	297.5 ± 0.5	0.8632 ± 0.0003	0.8889 ± 0.0051
5	20.32	363.6 ± 0.5	0.8248 ± 0.0003	0.8584 ± 0.0055

Next, the  $^{235}\text{U}$  enrichment was reduced to 80 wt% from the standard 93.2 wt% and the Monte Carlo calculations were repeated. The results of the analysis are presented in Table 5. Again the inferred keff value ranges were consistent with previous perturbations.

Table 5. Perturbed Spectral Ratio and  $k_{eff}$  Values and Experimental keff Obtained from Changing the  $^{235}\text{U}$  Enrichment to 80 wt% using ENDF/B-V Cross Sections

Case	Solution Height (cm)	Perturbed Spectral Ratio ( $R_p$ ) ( $10^{-3}$ )	Perturbed ( $k_p$ ) $k_{eff}$	“Experimental” $k_{eff}$
1	30.48	151.0 ± 0.1	0.9396 ± 0.0003	0.9632 ± 0.0053
2	27.94	192.7 ± 0.3	0.9192 ± 0.0003	0.9450 ± 0.0047
3	25.40	243.9 ± 0.3	0.8952 ± 0.0003	0.9224 ± 0.0049
4	22.86	299.0 ± 0.3	0.8640 ± 0.0003	0.8884 ± 0.0047
5	20.32	360.6 ± 0.4	0.8513 ± 0.0003	0.8589 ± 0.0057

The perturbations in the tank dimensions were also used to determine the inferred keff values as shown in Tables 6 and 7. The inferred keff values were consistent with those obtained from perturbing the solution density, uranium enrichment, and uranium density.

Table 6. Perturbed Spectral Ratio and  $k_{eff}$  Values and Experimental  $k_{eff}$  Obtained from Increasing the Tank Inner Radius by 0.15-cm using ENDF/B-V Cross Sections

Case	Solution Height (cm)	Perturbed Spectral Ratio ( $R_p$ ) ( $10^{-3}$ )	Perturbed ( $k_p$ ) $k_{eff}$	“Experimental” $k_{eff}$
1	30.48	$88.4 \pm 0.1$	$0.9672 \pm 0.0003$	$0.9631 \pm 0.0051$
2	27.94	$135.8 \pm 0.2$	$0.9462 \pm 0.0003$	$0.9447 \pm 0.0044$
3	25.40	$189.3 \pm 0.2$	$0.9213 \pm 0.0003$	$0.9236 \pm 0.0057$
4	22.86	$247.3 \pm 0.5$	$0.8897 \pm 0.0003$	$0.8893 \pm 0.0054$
5	20.32	$314.6 \pm 1.0$	$0.8513 \pm 0.0003$	$0.8568 \pm 0.0049$

Table 7. Perturbed Spectral Ratio and  $k_{eff}$  Values and Experimental  $k_{eff}$  Obtained from Decreasing the Tank Inner Radius by 0.15-cm using ENDF/B-V Cross Sections

Case	Solution Height (cm)	Perturbed Spectral Ratio ( $R_p$ ) ( $10^{-3}$ )	Perturbed ( $k_p$ ) $k_{eff}$	“Experimental” $k_{eff}$
1	30.48	$123.5 \pm 0.1$	$0.9517 \pm 0.0003$	$0.9633 \pm 0.0055$
2	27.94	$167.5 \pm 0.1$	$0.9310 \pm 0.0003$	$0.9453 \pm 0.0049$
3	25.40	$216.5 \pm 0.2$	$0.9072 \pm 0.0003$	$0.9232 \pm 0.0055$
4	22.86	$275.0 \pm 0.4$	$0.8761 \pm 0.0003$	$0.8879 \pm 0.0043$
5	20.32	$339.4 \pm 0.5$	$0.8379 \pm 0.0003$	$0.8594 \pm 0.0060$

The experimental  $k_{eff}$  values obtained from the various perturbation analyses agree closely. The variation is much less than the experimental uncertainty. The dependence of the interpreted experimental  $k_{eff}$  values on cross sections was investigated by performing calculations using the ENDF/B-VI and JENDL-3.2 cross section data sets. The results of the perturbation analysis for the 30.48-cm high solution are presented in Table 8 for ENDF/B-VI cross sections. The average experimental  $k_{eff}$  is  $0.9602 \pm 0.0051$  and is slightly less than the ENDF/B-V value of  $0.9631 \pm 0.0052$  for the 30.48-cm high solution. A similar perturbation analysis was performed using JENDL-3.2 neutron cross-section data. The results of the perturbation analysis for the 30.48-cm high solution are presented in Table 9 for JENDL-3.2 cross sections. The average experimental  $k_{eff}$  is  $0.9610 \pm 0.0050$  and is also slightly lower than the ENDF/B-V value of  $0.9631 \pm 0.0052$  for the 30.48-cm high solution. A more limited set of simulations was performed for each solution height. The results of these simulations were actually in better agreement than those for the 30.48-cm high solution.

Table 8. Spectral ratio and  $k_{eff}$  values for 30.48-cm high solution using ENDF/B-VI cross-section data set

Condition	Spectral Ratio ( $10^{-3}$ )	$k_{eff}$	“Experimental” $k_{eff}$
Base	$102.7 \pm 0.1$	$0.9582 \pm 0.0003$	N/A
+2% Solution Density	$61.1 \pm 0.1$	$0.9754 \pm 0.0003$	$0.9601 \pm 0.0050$
+3% Uranium Density	$147.3 \pm 0.1$	$0.9392 \pm 0.0003$	$0.9603 \pm 0.0054$
-3% Uranium Density	$73.9 \pm 0.1$	$0.9713 \pm 0.0003$	$0.9602 \pm 0.0051$
80 wt% $^{235}\text{U}$	$149.3 \pm 0.1$	$0.9382 \pm 0.0003$	$0.9602 \pm 0.0051$
+0.15-cm ID	$85.1 \pm 0.1$	$0.9664 \pm 0.0003$	$0.9604 \pm 0.0056$
-0.15-cm ID	$120.5 \pm 0.1$	$0.9511 \pm 0.0003$	$0.9601 \pm 0.0048$
Average	N/A	N/A	$0.9602 \pm 0.0052$

Table 9. Spectral ratio and  $k_{eff}$  values for 30.48-cm high solution using JENDL-3.2 cross-section data set

Condition	Spectral Ratio ( $10^{-3}$ )	$k_{eff}$	“Experimental” $k_{eff}$
Base	$84.5 \pm 0.1$	$0.9666 \pm 0.0003$	N/A
+2% Solution Density	$41.6 \pm 0.1$	$0.9837 \pm 0.0003$	$0.9612 \pm 0.0048$
+3% Uranium Density	$131.3 \pm 0.1$	$0.9470 \pm 0.0003$	$0.9609 \pm 0.0050$
-3% Uranium Density	$35.6 \pm 0.1$	$0.9862 \pm 0.0003$	$0.9612 \pm 0.0048$
80 wt% $^{235}\text{U}$	$132.8 \pm 0.1$	$0.9460 \pm 0.0003$	$0.9608 \pm 0.0051$
+0.15-cm ID	$65.5 \pm 0.1$	$0.9750 \pm 0.0003$	$0.9606 \pm 0.0053$
-0.15-cm ID	$102.8 \pm 0.1$	$0.9592 \pm 0.0003$	$0.9611 \pm 0.0048$
Average	N/A	N/A	$0.9610 \pm 0.0050$

## 5. CONCLUSIONS

The analysis of the uranyl nitrate solution measurements has demonstrated that the interpretation of source-driven noise analysis measurements using the perturbation method is robust. The interpreted  $k_{eff}$  values from the perturbation analysis were shown to be independent of the perturbation made to the system and were also shown to be essentially independent of the nuclear cross section data set. The largest difference between the interpreted  $k_{eff}$  values was 0.003 for the three data sets used in this analysis. This slight difference is well within the uncertainty of the measured quantities.

## ACKNOWLEDGEMENTS

Based on work performed at Oak Ridge National Laboratory, operated for the U.S. Department of Energy under contract DE-AC05-00OR22725 with Oak Ridge National Laboratory, managed by UT-Battelle, LLC.

## REFERENCES

1. V. K. Paré and J. T. Mihalczo, "Reactivity from Power Spectral Density Measurements with Californium-252," *Nucl. Sci. Eng.* **56**, 213 (1975).
2. J. L. Muñoz-Cobo and G. Verdu, "Neutron Stochastic Transport Theory with Delayed Neutrons," *Annals Nuclear Energy* **14**, 7,327 (1987).
3. T. E. Valentine, "MCNP-DSP Users Manual", ORNL/TM-13334-R2, Oak Ridge Nat. Lab, October 2000.
4. R. B. Perez, T. E. Valentine, J. T. Mihalczo, and J. K. Mattingly, "Determination of the Multiplication Factor and Its Bias by the  $^{252}\text{Cf}$ -Source Technique: A Method for Code Benchmarking at Subcritical Configurations," *Proc. Topical Meeting of the Am. Nucl. Soc.*, Saratoga, N. Y. (1997).
5. T. E. Valentine, *Review of Subcritical Source-Driven Noise Analysis Measurements*, ORNL/TM-1999/288, Lockheed Martin Energy Research Corp., Oak Ridge National Laboratory, November 1999.
6. J. T. Mihalczo, E. D. Blakeman, G. E. Ragan, E. B. Johnson, Y. Hachiya, "Dynamic Subcriticality Measurements Using the  $^{252}\text{Cf}$ -Source-Driven Noise Analysis Method," Oak Ridge National Laboratory, ORNL/TM-10122 (1988).
7. "International Handbook of Evaluated Criticality Safety Benchmark Experiments," NEA/NSC/DOC (95) 03, Nuclear Energy Agency, Organization for Economic Cooperation and Development (Sep. 2000).

The submitted manuscript has been authored by a contractor of the U. S. government under contract DE-AC05-00OR22725. Accordingly, the U. S. Government retains a nonexclusive, royalty free license to publish or to reproduce the published form of this contribution, or allow others to do so, for U. S. Government purposes.